As a solution to these problems, a novel cell separation system was designed based on the cell-rolling process that can separate cells with a given surface marker density. First reported by Andrian in 1991, the leukocyte-rolling mechanism has been defined as the temporal interaction between a leukocyte surface marker and endothelial cells on the blood vessel luminal surfaces.[18] Hammer et al. described the temporal interaction between the cell surface markers and the immobilized ligand in the flow media.[19] Detailed mechanisms of the rolling adhesion properties of cells have been reported by other groups.[20–25] This unique concept has also been applied in drug screening,[26] local delivery of therapeutics,[27] and studies of cell regulation.[22,28,29] Antibody-immobilized microfluidic devices and microfabricated-cell sorters have been developed for isolating target cells with an adequate surface marker using the positive/negative selection method.[30,31] Patterning surface of receptors has been used as a means of continuous separation of cells by cell rolling.[32] This mechanism effectively isolates large quantities of cells. However, the cells in this system are intermittently rolled on the surface, and cell rolling as well as tethering between the receptor-coated region and the unmodified region are induced by the pattern and its edge. This surface approach is also an effective method of cell separation by cell rolling.

In this study, we focused on whether CD34-positive cells could be finely separated based on the CD34 densities on their surface. The KG-1a cell line, which is CD34-positive, was used as the model, while the CD34-negative HL-60 cell line was used as the control. We developed a tubular column with a continuous surface for cell separation such that the anti-CD34 antibody was immobilized at a high density on the surface. Chemical immobilization of the antibody through poly(acrylic acid) graft polymerization prevents antibody contamination of the purified cells. The injected cells are rolled on the inner surface of the column due to the medium flow shear force, in a manner similar to that of the rolling adhesion process of a leukocyte in a blood vessel.[18] The cell suspensions of KG-1a or HL-60 were passed through the column, and the cell numbers and the surface marker pattern on the cells were evaluated in each elution fraction.

Materials and Methods

Culturing of KG-1a and HL-60 cells

CD34-positive KG-1a cells were grown in IMEM culture medium (Invitrogen, Carlsbad, CA) supplemented with 10% fetal bovine serum (FBS) (Sigma, St. Luis, MO), penicillin (100 U/mL), and streptomycin (100 μg/mL). CD34-negative HL-60 cells were grown in RPMI medium (Invitrogen, Carlsbad, CA) containing 20% FBS with antibiotics. The cell lines were cultured in a humidified atmosphere containing 5% CO_2 at 37°C.

Antibody-immobilized column

Polyethylene tubes with a 1-mm inner diameter were selected as the substrate for the cell-separation column. Graft polymerization of acrylic acid onto the column was conducted as follows. The tube was treated with ozone gas (ON-3-2, Nippon Ozone Co.Ltd., Tokyo, Japan) for 4 h, dipped in 0–30% acrylic acid/methanol solution, and incubated at 60°C. After 4 h, the tube was washed with water.[33,34] The graft polymerization was confirmed by toluidine blue staining. To immobilize the anti-CD34 antibody on the tube surface, the poly(acrylic acid)-grafted tube was activated using 1-ethyl-3-(3-dimethylaminopropyl) carbodiimide hydrochloride (WSC) under various conditions. Thereafter, the activated tube was filled with a 0.1 mg/mL solution of the monoclonal mouse anti-human CD34 class II antibody (Dako Ltd., Carpenteria, CA), and incubated at 37°C for 15 h. The tube was washed with PBS, treated with 1 mM 2-aminoethanol solution for 1 h and preserved at 4°C until experimental use. The antibody density on the luminal surface was evaluated using peroxidase conjugated anti-mouse IgG (whole molecule) antibody (Sigma, St. Luis, MO). Peroxidase activity was measured using the SMILON Peroxidase Detection Kit (Sumitomo Bakelite Co.,Ltd., Tokyo, Japan).

Separation of cells on the antibody-immobilized column

The antibody-immobilized column was connected using a syringe pump (Model:780120J; KD Scientific Inc., Holliston, MA) through the unmodified tube. The length of the antibody-immobilized column and the unmodified tube was 100 mm, and the cell suspension was directly injected into the unmodified tube using a disposable syringe with a 27 G needle. The column was inclined against the ground, and the tilt angle was fixed by clamping. Cell separation was performed as follows. The KG-1a or HL-60 cell suspension (2×10^4 cells/50 μL) was injected into the column. After injection, PBS buffer was flushed into the column to promote cell rolling on the surface. The flow rate of PBS was optimized by experimentation. The eluted cell suspension was then collected from the end of the column; collected volume of each fraction was 50 μL. The numbers and surface marker profiles of the eluted cells were analyzed using FACS.

Rolling velocity of the KG-1a cells

The microfluidic device was purchased from ibidi GmbH (Model ib80501; ibidi GmbH, Martinsried, Germany). The dimensions of the microfluidic channel were 24 mm (length) × 500 μm (width) × 300 μm (height), with one inlet and one outlet. Anti-CD34 antibody was immobilized on the channel surface, and the modification method used was the same as that used for the tubular column. The cell suspension (2×10^6 cells/mL) was injected into the inlet at a rate of 50 μL/min, and cell rolling was recorded using a high-speed CCD camera (EM-CCD digital camera; Hamamatsu,

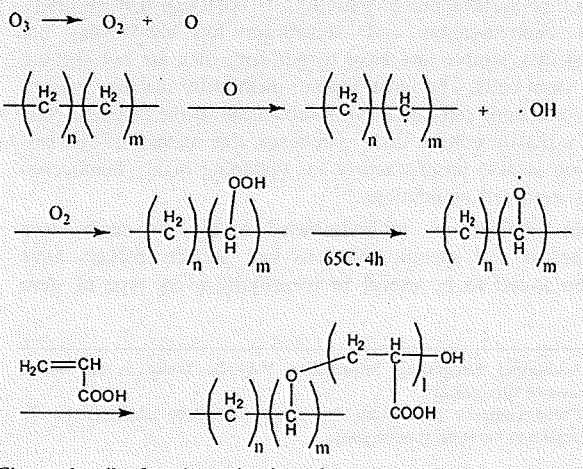

Figure 1. Graft polymerization of acrylic acid on the polyethylene tube.

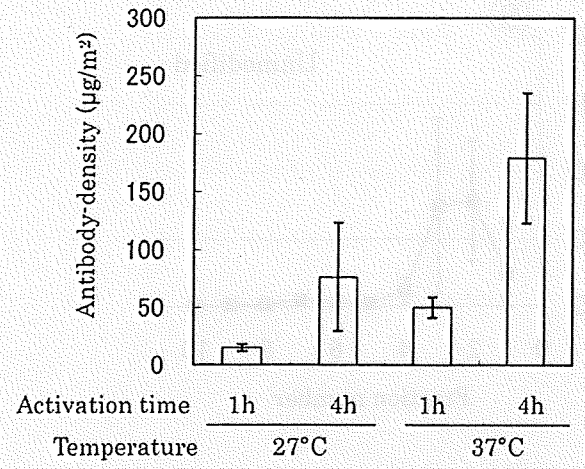

Figure 2. Effects of reaction conditions on immobilized antibody density.

The degree of immobilization is substantially affected by the duration and temperature of the WSC activation reaction. Each data point represents the results of three independent experiments. Data are presented as means ± standard error on the mean.

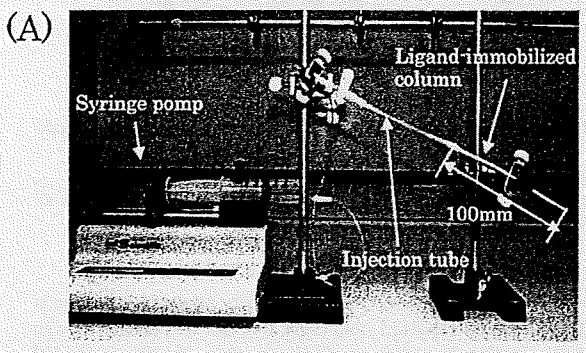

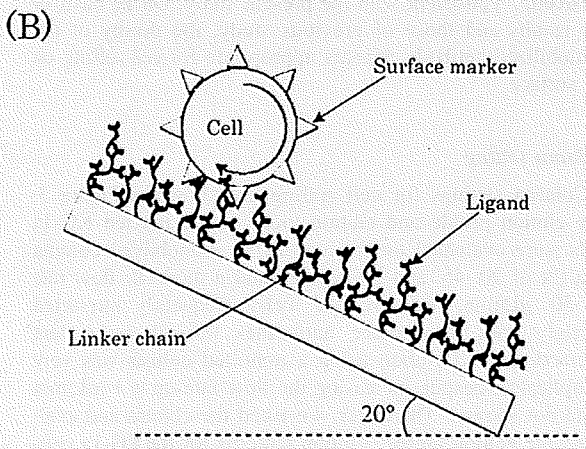

Figure 3. (A) Photograph of the cell separation column system. The antibody-immobilized column was connected to the injection tube and syringe pump. Cells were injected into the injection tube and PBS continuously flowed into the column. The eluted fraction was collected at the end of the column. (B) Schematic diagram of cell rolling on the antibody-immobilized column.

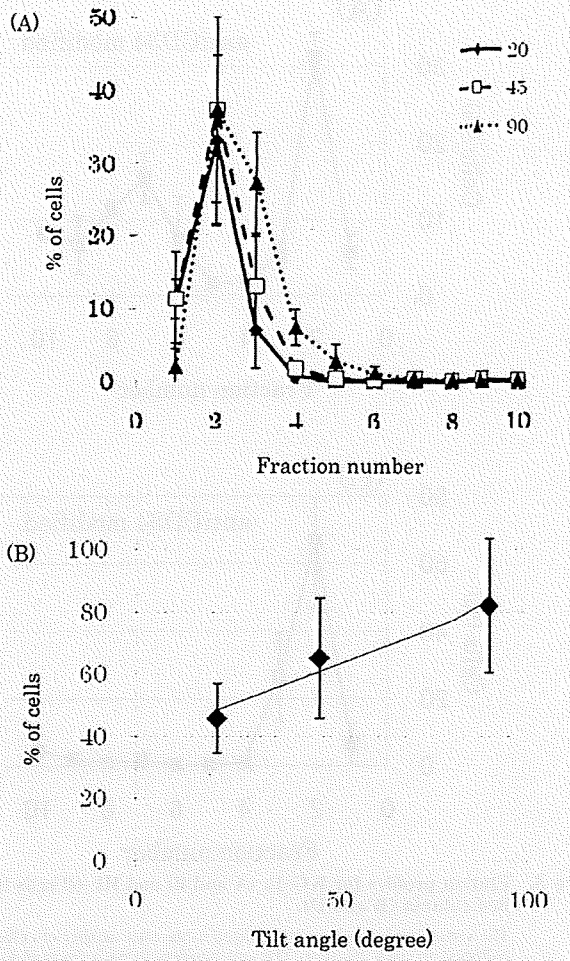

Figure 4. (A) Elution pattern for KG-1a cells at different tilt angles of the antibody-immobilized column, and (B) elution yield of injected KG-1a cells. The vertical axis has been normalized to the total number of injected KG-1a cells. Each data point represents the results of three independent experiments.

Hamamatsu city, Japan). The motion and velocity were analyzed using a personal computer.

FACS analysis

Isolated cells were incubated with FITC-conjugated anti-human CD34 monoclonal antibody (BD Bioscience, San Diego, CA) in PBS for 30 min at 4°C and analyzed using a FACS-Calibur Flow Cytometer (BD Bioscience, San Jose, CA).

Results and Discussion

Fabrication of the antibody-immobilized column

Ozone-induced graft polymerization is effective for polyethylene matrices with a fine structure because ozone gas can be charged into the inner surface and peroxides can be uniformly introduced. The reaction mechanism is shown in Figure 1. The surface concentration of peroxide and its reaction mechanism with vinyl monomer have been previously reported.[33,34] The introduction of the graft polymer chain was confirmed by toluidine blue staining. When the polymer

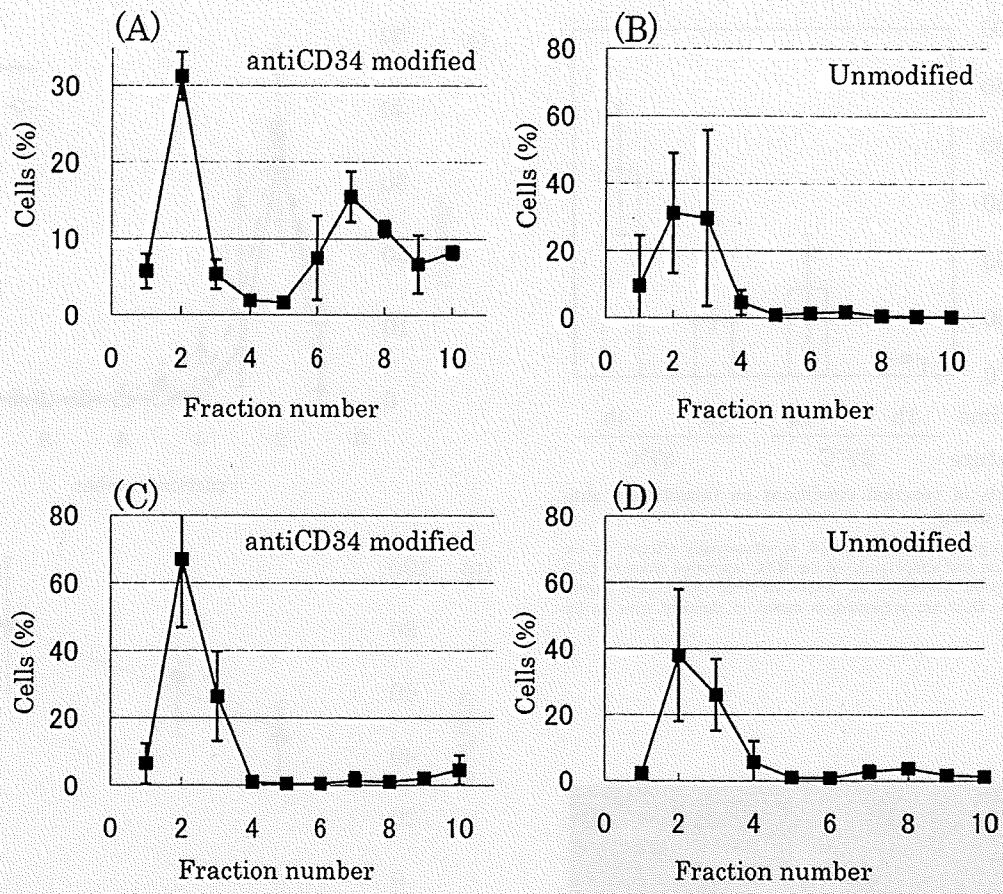

Figure 5. Elution profiles for KG-1a (A and B) and HL-60 cells (C and D) on the anti-CD34 modified column (A and C) and unmodified column (B and D).

The vertical axis has been normalized to the total number of cells. Fifty microliters of the cell suspension was applied and 50 μL of the eluant was collected in each fraction. The cell numbers in each fraction were analyzed using FACSCalibur flow cytometry. Each data point represents the results of 3 independent experiments; the data are presented as means ± standard error on the mean.

concentration was 30%, it was more difficult to flash medium inside the column compared with the lower concentrations. Therefore, a column reacted with 20% acrylic acid solution was selected for the subsequent experiments.

To develop a high-performance column for separating cells with various surface marker densities, the density of the immobilized anti-CD34 antibody should be well controlled. To optimize conditions for antibody immobilization on the inner surface of the tube, we measured the density of the immobilized antibody using HRP-labeled anti-mouse IgG goat antibody. Figure 2 shows the effects of temperature and the WSC activation period on the immobilized density of the anti-CD34 antibody. At an activation temperature of 27°C, the antibody could not be immobilized to the graft chain. On the other hand, when the reaction mixture was incubated at 37°C, the density of the immobilized antibody was approximately 180 $\mu g/m^2$ or about 1.2×10^9 mol/m^2. Cell rolling adhesion is defined as the continuous interaction between a ligand and the cell surface.[18] Rolling velocity is largely restricted by the ligand density and the interaction with the surface marker. Greenberg reported that 10^9 mol/m^2 (800 sites/μm^2) was suitable for cell rolling on a ligand-modified substrate in an experimental as well as theoretical study.[22] In our experiments, the anti-CD34 antibody density in the area occupied by a single cell was 6.3×10^4 sites/cell, and the antibody density was nearly the same as that in Greenberg's report. On the basis of QuantiBrite PE analysis, Zborowski and coworkers reported that Jurkat cells expressed a high number of CD45 surface antigens with a density of 9×10^4 sites/cell,[35] consistent with the present study. On the basis of our results and those of previous study, the density of the immobilized antibody appears appropriate for cell rolling on the surface.

Column setting

Column settings for cell rolling are shown in Figure 3. The elution profile and elution yield of the injected KG-1a cells were evaluated on the anti-CD34 immobilized column at a tilt of 20, 45, and 90 degrees and a moderate flow rate of 50 μL/min. Because the cells frequently interacted strongly with the surface antibodies through multivalent interactions, cell elution using a nontilted column was very complicated, despite increasing the flow rate up to 1 mL/min (data not shown). Thereafter, we tilted the column and evaluated the elution profile. Elution patterns for the KG-1a cells at various tilt angles of the column were almost the same, with a single elution peak observed at Fraction 2 (Figure 4A). The injected cells were almost completely eluted without any surface interactions at an angle of 90 degrees. However, the total recovery ratio of the injected cells decreased with decrease in tilt angle (Figure 4B). When the column

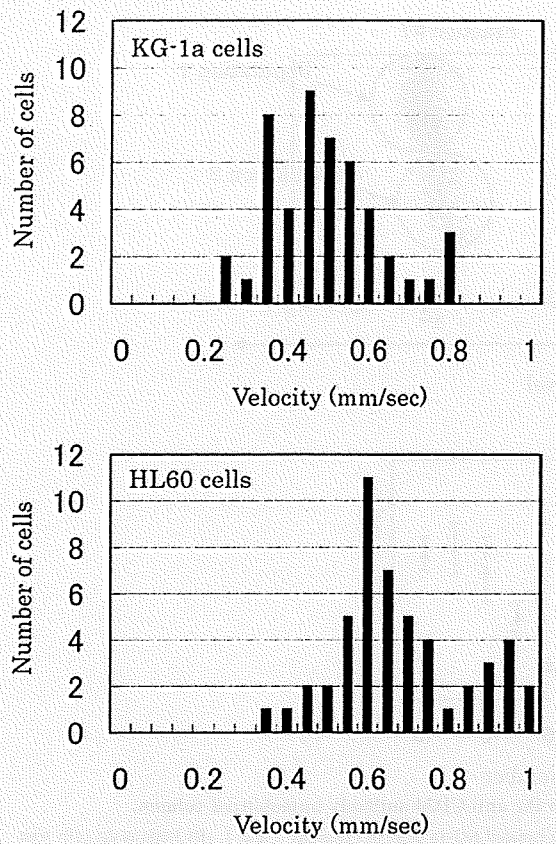

Figure 6. Distributions of the rolling velocities of KG-1a and HL-60 cells on the anti-CD34 antibody immobilized surface. Rolling cells were monitored using a high-speed CCD camera.

angle was 20 degrees, half of the injected cells remained in the column. It is likely that these cells interacted with the surface antibodies, thereby greatly reducing the rolling velocity. After flushing at 50 μL/min, the flow rate was changed to 600 μL/min and most of the injected cells were eluted. We tilted the column angle to 20 degrees, and thus, the cells that interacted with the antibody-immobilized surface rolled on the surface with higher velocity because of the increase in the flow rate. The initial flow rate was maintained at 50 μL/min through Fraction 5, and the rate was changed to 600 μL/min thereafter.

Specificity of the separation profile

KG-1a cells could be separated using the antiCD34 antibody-immobilized column with the settings described earlier. A bimodal elution pattern was observed (Figure 5A). The first elution peak corresponded to the single peak in Figure 4A, suggesting that the cells in the first peak did not interact with the immobilized antibody. In contrast, the delayed fraction was not observed when the KG-1a cells were injected into the unmodified column (Figure 5B). Elution profiles for HL-60 cells (CD34-negative) were compared with those for the CD34-positive cells. All injected HL-60 cells were eluted from the anti-CD34 antibody-immobilized and unmodified column in Fractions 1–3 (Figure 5C,D). This elution profile was the same as the pattern resulting from the column angle fixed at 90 degrees (Figure 4A); that is, HL60 cells injected into the column did not interact with the immobilized antibody. This indicates that the retention time of the cells in the delayed fraction depends on the specific interaction between the surface marker and the immobilized antibody (Supporting Information).

Additional evidence of successful cell separation using the cell rolling mechanism on the column was provided by observation of the rolling velocities on the antibody-immobilized surface. We used a microfluidic channel to measure the distribution of rolling velocities. The microfluidic channel, which was modified with anti-CD34 antibody in the same manner as the column, was set on a microscopy stage, and cell rolling was monitored using a high-speed CCD camera at a moderate flow rate of 50 μL/min. Some cells adhered onto the antibody-immobilized surface and were not able to flow again after adhesion due to multivalent interaction between the cell surface and immobilized antibody. The velocities of the KG-1a and HL-60 rolling cells on the anti-CD34 antibody-immobilized microchannel were 0.45 mm/s and 0.6 mm/s, respectively (Figure 6). Conditions for measurement of the cell rolling velocity on the microscope were different from the cell separation experiments, because the microfluidic device was placed on the flat stage of the microscope without a tilt angle. Under these conditions, large differences in rolling velocity between KG-1a and HL-60 cells were not observed (Figure 6). However, the distributions of the velocities were distinctly different between the KG-1a and HL-60 cells. The difference in the interactions is likely reflected in the velocity distributions. Thus, the velocity of cells rolling was largely dependent on the cell surface marker.

Hammer et al. reported that the rolling velocity of saturated sLe^x-modified polystyrene microspheres was 20 times slower than that of microspheres with a low surface density of sLe^x on an L-selectin coated surface; this difference could be successfully exploited for separation.[8,9] However, it was also reported that CD34-positive bone marrow cells rolled only twice as slowly as CD34-negative cells on an L-selectin modified surface. We observed similar differences in rolling velocities between CD34-positive and -negative cells on the antibody-immobilized surfaces. This small difference in the rolling velocity on a flat microfluidic device prevented cell separation, as shown in Figure 5. We optimized a variety of separation conditions such as consideration of the surface modification tendency, changes in the medium flow rate, and modifying the column setting conditions; this resulted in the bimodal pattern shown in Figure 5A. In our system, separation of rolling cells was most effective after optimization of the column tilt angle and flow rate.

Surface marker characteristics of the isolated cells

To confirm whether our column could be used to separate cells based on CD34 surface density, the CD34 expression level of the KG-1a cells in each fraction was investigated by dual dimensional FACS analysis. Forward-light scatter characteristics (FSC) depend on cell size, which is related to cell cycle or cell proliferation. Fluorescence intensity, indicating the CD34 expression level of each cell line for fractions 2 and 7, is shown in Figure 7A. Two populations of KG-1a were identified by the FACS analysis of CD34 expression versus FSC signal. Although a single population was indicated by the FACS data for Fraction 2, two cell populations (Populations 1 and 2) were observed in Fraction 7. The CD34 expression level of Population 1 was nearly the same as for Population 2, but the cell size of Population 2 was

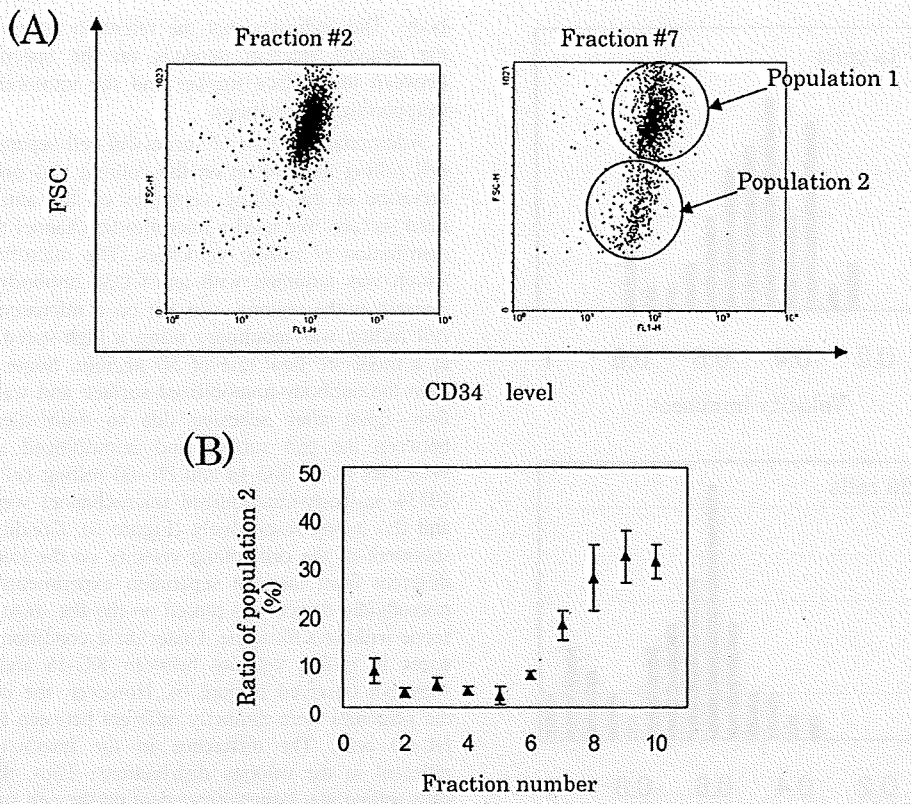

Figure 7. Analysis of the surface marker density of isolated KG-1a cells on the anti-CD34 antibody immobilized column.

(A) Dual dimensional analysis of the CD34 expression level and FSC of the isolated KG-1a cells in Fractions 2 and 7. (B) Ratio of the cells with population producing a high concentration of CD34 in each fraction. Each data point represents the results of three independent experiments.

about half of Population 1. Therefore, the density of CD34 in Population 2 was about 4 times higher than that of Population 1. In Fraction 2, a majority of the cells were of Population 1 as the cell rolling velocity was much larger than for Population 2. The population of the CD34-dense populations was plotted against the fraction number (Figure 7B), and gradually increased with elution time. If the cells in the delayed fraction were separated by static adhesion onto the surface, the high CD34-expression population could not have been isolated from the CD34-positive cell population, because all of the injected cells would have adhered to the resulting surface (Figure 4A). These findings suggest that the cells in the delayed fraction rolled more slowly on the surface than the cells in the previous fractions in a marker-specific manner under shear flow conditions. Thus, this separation procedure is able to isolate cell populations with different marker densities in a continuous manner.

Conclusions

Development of an effective cell separation system is crucial for cell transplantation and for the fundamental study of cell biology. In many cases, negative or positive selection has been used as an effective strategy for cell separation, and the MACS system is a suitable technology for conducting the selection. However, this system cannot separate cells with different densities of surface markers. On the other hand, FACS system can separate cells based on the marker expression level, cellular density, and cell size. For these reasons, FACS was effective in separating the cells in Population 1 and 2 of the KG-1a cells. In this study, we demonstrated the feasibility of a novel cell-separation column that isolates cells through the cell rolling process based on surface marker density under labeling-free conditions. In the standard FACS system, the cells would be exposed to strong media flow, and its velocity and antibody labeling would reduce its viability. To improve the purity of the cells isolated by the column, it is necessary to optimize the surface antibody modification and column structure.

Our system offers several advantages over conventional methods. We would expect cell separation to be more rapid than with conventional methods; moreover, an antibody-immobilized column would likely reduce the degree of cellular damage because cell modification using fluorescence- or magnetic beads-labeled antibodies is unnecessary. For the same reason, the cells thus purified are free of contamination. A highly purified cell population without such impurities or additives will provide an important tool for both transplantation therapy and fundamental study.

Acknowledgments

This work was supported by the Research Grant for Cardiovascular Disease (18A-2) from the Ministry of Health, Labour and Welfare & Grant-in-Aid for Scientific Research on Innovative Areas (20106014).

Literature Cited

1. Stamm C, Westphal B, Kleine HD, Petzsch M, Kittner C, Klinge H, Schumichen C, Nienaber CA, Freund M, Steinhoff G. Autologous bone-marrow stem-cell transplantation for myocardial regeneration. *Lancet*. 2003;361:45–46.

2. Pittenger MF, Martin BJ. Mesenchymal stem cells and their potential as cardiac therapeutics. *Circ Res.* 2004:95:9–20.
3. Noishiki Y, Tomizawa Y, Yamane Y, Matsumoto A. Autocrine angiogenic vascular prosthesis with bone marrow transplantation. *Nat Med.* 1996:2:90–93.
4. Shin'oka T, Imai Y, Ikada Y. Transplantation of a tissue-engineered pulmonary artery. *N Engl J Med.* 2001;344:532–533.
5. Gronthos S, Zannettino ACW, Hay SJ, Shi S, Graves SE, Kortesidis A, Simmons PJ. Molecular and cellular characterisation of highly purified stromal stem cells derived from human bone marrow. *J Cell Sci.* 2003:116:1827–1835.
6. Hung S-C, Chen N-j, Hsieh S-L, Li H, Ma H-L, Lo W-H. Isolation characterization of size-sieved stem cells from human bone marrow. *Stem Cells.* 2002;20:249–258.
7. Pittenger MF, Mackay AM, Beck SC, Jaiswal RK, Douglas R, Mosca JD, Moorman MA, Simonetti DW, Craig S, Marshark DR. Multilineage potential of adult human mesenchymal stem cells. *Science.* 1999:284:143–147.
8. Reyes M, Lund T, Lenvik T, Aguiar D, Koodie K, Verfaillie CM. Purification and ex vivo expansion of postnatal human marrow mesodermal progenitor cells. *Blood.* 2001;98:2615–2625.
9. Jiang Y, Jahagirdar BN, Reinhardt RL, Schwartz RE, Keene CD, Ortiz-Gonzalez XR, Reyes M, Lenvik T, Lund T, Blackstad M, Du J, Aldrich S, Lisberg A, Low WC, Largaespada DA, Verfaillie CM. Pluripotency of mesenchymal stem cells derived from adult marrow. *Nature.* 2002;418:41–49.
10. Baddoo M, Hill K, Wilkinson R, Gaupp D, Hughes C, Kopen GC, Phinney DG. Characterization of mesenchymal stem cell isolated from murine bone marrow by negative selection. *J Cell Biochem.* 2003:89:1235–1249.
11. Gojo S, Gojo N, Takeda Y, Mori T, Abe H, Kyo S, Hata J, Umezawa A. In vivo cardiovasculogenesis by direct injection of isolated adult mesenchymal stem cells. *Exp Cell Res.* 2003; 288:51–59.
12. Tropel P, Noël D, Platet N, Legrand P, Benabid AL, Berger F. Isolation and characterisation of mesenchymal stem cells from adult mouse bone marrow. *Exp Cell Res.* 2004;295:395–406.
13. Rafii S, Lyden D. Therapeutic stem and progenitor cell transplantation for organ vascularization and regeneration. *Nat Med.* 2003;9:702–712.
14. Ziegler BL, Valtieri M, Porada GA, De Maria R, Muller R, Masella B, Gabbianelli M, Casella I, Pelosi E, Bock T, Peschle C. KDR receptor: a key marker defining hematopoietic stem cells. *Science.* 1999;285:1553–1558.
15. Li Y, Zhang C, Xiong F, Yu MJ, Peng FL, Shang YC, Zhao CP, Xu YF, Liu ZS, Zhou C, Wu JL. Comparative study of mesenchymal stem cells from C57BL/10 and mdx mice. *BMC Cell Biol.* 2008:9:24.
16. Jankowski RJ, Deasy BM, Cao B, Gates C, Huard J. The role of CD34 expression and cellular fusion in the regeneration capacity of myogenic progenitor cells. *J Cell Sci.* 2002;115: 4361–4374.
17. Matsuoka S, Ebihara Y, Xu M, Ishii T, Sugiyama D, Yoshino H, Ueda T, Manabe A, Tanaka R, Ikeda Y, Nakahata T, Tsuji K. CD34 expression on long-term repopulating hematopoietic stem cells changes during developmental stages. *Blood.* 2001; 97:419–425.
18. Von Andrian UH, Chambers JD, Mcevoy LM, Bargatze RF, Arfors KE, Butcher EC. Two-step model of leukocyte-endothelial cell interaction in inflammation: distinct roles for LECAM-1 and the leukocyte beta 2 integrins in vivo. *Proc Natl Acad Sci USA.* 1991:88:7538–7542.
19. Hammer DA, Lauffenburger DA. A dynamical model for receptor-mediated cell adhesion to surfaces. *Biophys J.* 1987:52: 475–487.
20. Cozens-Roberts C, Quinn JA, Lauffenberger DA. Receptor-mediated adhesion phenomena. Model studies with the radial-flow detachment assay. *Biophys J.* 1990;58:107–125.
21. Reinhardt PH, Kubes P. Differential leukocyte recruitment from whole blood via endothelial adhesion molecules under shear conditions. *Blood.* 1998;92:4691–4699.
22. Greenberg AW, Kerr WG, Hammer DA. Relationship between selectin-mediated rolling of hematopoietic stem and progenitor cells and progression in hematopoietic development. *Blood.* 2000:95:478–486.
23. Greenberg AW, Brunk DK, Hammer DA. Cell-free rolling mediated by L-selectin and sialyl Lewis(x) reveals the shear threshold effect. *Biophys J.* 2000;79:2391–2402.
24. King MR, Hammer DA. Multiparticle adhesive dynamics. Interactions between stably rolling cells. *Biophys J.* 2001; 81:799–813.
25. Hanley WD, Wirtz D, Konstantopoulos K. Distinct kinetic and mechanical properties govern selectin-leukocyte interactions. *J Cell Sci.* 2004:117:2503–2511.
26. Salimi-Moosavi H, Szarka R, Andersson P, Smith R, Harrison DJ. Biology Lab-on-a-Chip for Drug Screening, Canada. *Proceedings Micro Total Analysis Systems '98.* 1998.
27. Omolola Eniola A, Hammer DA. In vitro characterization of leukocyte mimetic for targeting therapeutics to the endothelium using two receptors. *Biomaterials.* 2005;26:7136–7144.
28. Greenberg AW, Hammer DA. Cell separation mediated by differential rolling adhesion. *Biotechnol Bioeng.* 2001:73:111–124.
29. Chang WC, Lee LP, Liepmann D. Biomimetic technique for adhesion-based collection and separation of cells in a microfluidic channel. *Lab Chip.* 2005:5:64–73.
30. Fu AY, Spence C, Scherer A, Arnold FH, Quake SR. A microfabricated fluorescence-activated cell sorter. *Nat Biotechnol.* 1999:17:1109–1111.
31. Miwa J, Suzuki Y, Kasagi N. Adhesion-based cell velocity regulation in an antibody-coated micro column for stem cell separation. In: *Nineth International Conference in Miniaturezed System Chemistry and Life Science*, Boston; 2005:868–870.
32. Karnik R, Hong S, Zhang H, Mei Y, Anderson DG, Karp JM, Langer R. Nanomechanical control of cell rolling in two dimensions through surface patterning of receptors. *Nano Lett.* 2008; 8:1153–1158.
33. Fujimoto K, Takebayashi Y, Inoue H, Ikada Y. Ozone-induced graft polymerization onto polymer surface. *J Polym Sci Part A: Polym Chem.* 1993;31:1035–1043.
34. Yamauchi J, Yamaoka A, Ikemoto J, Matsui T. Graft copolymerization of methyl methacrylate onto polypropylene oxidized with ozone. *J Polym Sci Part A: Polym Chem.* 1991;43:1197–1203.
35. Schneider T, Moore LR, Jing Y, Haam S, Williams PS, Fleischman AJ, Roy S, Chalmers JJ, Zborowski M. Continuous flow magnetic cell fractionation based on antigen expression level. *J Biochem Biophys Methods.* 2006;68:1–21.

Manuscript received Apr. 23, 2009, and revision received Aug. 18, 2009.

Biomaterials 31 (2010) 4231–4237

Contents lists available at ScienceDirect

Biomaterials

journal homepage: www.elsevier.com/locate/biomaterials

Continuous separation of cells of high osteoblastic differentiation potential from mesenchymal stem cells on an antibody-immobilized column

Atsushi Mahara [1], Tetsuji Yamaoka*

Department of Biomedical Engineering, Advanced Medical Engineering Center, National Cardiovascular Center Research Institute, Suita, Japan

ARTICLE INFO

Article history:
Received 24 December 2009
Accepted 21 January 2010
Available online 24 February 2010

Keywords:
Mesenchymal stem cells
Selection
Interface
Osteoblast

ABSTRACT

Here, we report that two distinctive cell populations with osteoblastic differentiation ability were found in adherent cell populations from bone marrow. Mesenchymal stem cells (MSCs) were conventionally isolated by using adherent property of bone marrow cells onto a plastic culture dish. MSCs enriched on the basis of their adherent property were considered phenotypically and functionally heterogeneous. We developed a ligand-immobilized surface for separating subpopulation of adherent cells derived from bone marrow by the cell rolling process. We successfully isolate two cell populations with high differentiation ability for osteoblasts in adherent bone marrow cells by using the anti-CD34 antibody-immobilized column. The antibody was covalently conjugated with polyacrylic acid and introduced onto the inner surface of a silicone tube. When cell suspension of MSCs was injected into the antibody-immobilized column, different cell populations were isolated. After the cultivation of isolated cells in the osteoblastic differentiation medium for 1 week, few sub-populations were strongly induced to form osteoblastic cells. This study revealed that the ligand-immobilized surface can be used to continually separate cell populations under a labeling-free condition.

1. Introduction

It is widely known that adherent cells found in bone marrow have an ability to differentiate into osteoblasts, adipocytes and chondrocytes. That stem cell is generally named as marrow stromal cells or mesenchymal stem cells (MSCs). Cell differentiation property and its mechanisms have been widely studied in clinical and biological fields. In particular, the field of regenerative medicine focuses on tissue derived stem cells for autologous cell transplantation [1,2]. One important finding is that MSCs, which exist in not only bone marrow but also cord blood and adipose tissue, have therapeutic potential for heart, neural, and brain diseases [3–5]. A standard procedure for isolation of MSCs was reported by Pittenger et al. [6]. MSCs are easily separated by using the adherent property of bone marrow cells onto plastic culture dishes. Ficoll-Hypaque density gradient centrifugation is also used for separating mononuclear cells containing MSCs [7,8]. Other isolation methods based on selection of non-adherent cell population [9], STRO-1 antibody-recognized antigen level [10], and size-sieved cell population [11] have been reported. Isolation methods based on various combinations of cell surface markers have been reported by many groups [12–16].

Although the adherent property of MSCs has been widely used for their isolation, MSCs enriched on the basis of their adherent property are considered as phenotypically and functionally heterogeneous [17]. Surface marker characteristics such as marker density and its variation change with the differentiation process and development of MSCs. Surface marker profile of murine MSCs significantly differ with the passage levels [18,19]. CD34 expression of hematopoietic stem cells continuously decreases with the developmental stage [20]. Consequently, the development of a new approach to isolate MSCs population is important for homogeneous separation.

We have recently developed an antibody-immobilized column which can separate CD34-positive KG-1a cells from CD34 negative HL60 cell [21]. The separation mechanism seems to be based on dynamic interaction between cell surface marker (CD34) and immobilized antibody, known as the cell rolling. In nature, cell rolling is mainly observed in blood vessels as an inflammatory response of leukocytes [22], and its mechanism is derived from temporary interaction between cell surface and ligands. Rolling velocity is regulated by the ligand or cell surface receptor density [23–27]. Thus, cells with different rolling velocities are separated on the surface constantly modified with the ligand against a specific cell surface marker. This separation technique would

* Corresponding author. Tel.: +81 6 6833 5012x2637; fax: +81 6 6835 5476.
E-mail addresses: mahara@ri.ncvc.go.jp (A. Mahara), yamtet@ri.ncvc.go.jp (T. Yamaoka).
[1] Tel.: +81 6 6833 5012x2621; fax: +81 6 6835 5476.

0142-9612/$ – see front matter © 2010 Elsevier Ltd. All rights reserved.
doi:10.1016/j.biomaterials.2010.01.126

principally enable a labeling-free process, and the isolated cells are not contaminated with fluorescent or magnetic-labeled antibody. This procedure would be effective in separating sub-populations of MSCs with different density of surface marker.

In the present study, we applied the antibody-immobilized column to heterogeneous which acquired from murine bone marrow by conventional isolation procedures, and successfully found two different populations in the crude MSCs. The fractions of MSCs were cultured under an osteoblastic differentiation condition for 1 week, and gene expression of specific markers was analyzed by real-time polymerase chain reaction (PCR). To evaluate calcium deposition on the cells, staining with alizarine red S solution was carried out.

2. Materials and methods

2.1. Isolation and culture of mouse MSCs

MSCs were collected according to a protocol modified from Tropel et al. [16]. Mouse bone marrow cells (BMCs) were isolated by flushing the marrow cavities of 8–10-weeks-old C57Bl/6 mice (Japan SLC, Inc., Shizuoka, Japan). BMCs were cultured on a polystyrene cell culture dish (Iwaki Glass, Chiba, Japan) with alpha-MEM (Gibco-Invitrogen, Carlsbad, CA) containing 15% fetal bovine serum (FBS; MB Biomedicals, Inc., Eschwege, Germany), 25 U/ml penicillin, and 25 μg/ml streptomycin (Wako Pure Chemical Industries, Ltd., Osaka, Japan). Non-adherent cells were removed by replacing the culture medium after 3 days. The cells were grown to confluency, washed with the medium, and subcultured by using the Trypsin/EDTA kit (Lonza, Walkersville, MD). Confluent cells were plated at 1:2 to 1:3 dilutions. The adherent cells enriched into plastic culture dish with early passage (passage 3 or 4) were subjected to all experiment as crude MSCs.

2.2. Surface marker analysis and cell sorting by fluorescence activated cell sorting

To evaluate the expression of surface markers by fluorescence-activated cell sorting (FACS), cells were suspended in PBS buffer for 30 min at 4 °C with fluorescein- or phenylephrine-conjugated antibodies against the surface markers CD29, CD31, CD34, CD44, CD45, CD81, CD11b and Sca-1. Antibody labeling was performed using the standard protocol. CD29 and CD31 antibodies were purchased from AbD Serotec (Oxford, UK) and Immunotech (Marseille, France), respectively. CD34, CD11b and Sca-1 antibodies were purchased from eBiocience (San Diego, CA). CD44, CD45 and CD81 antibodies were purchased from Pharmingen (San Diego, CA). After labeling with antibodies, 10^4 cells were analyzed with a FACScalibur flow cytometer (BD Biosciences, San Jose, CA). Conventional sorting of cells with different CD34 expression levels was conducted by FACSAria (BD Biosciences), as control experiment.

2.3. Preparation of the anti-CD34 antibody-immobilized column

Silicone tubes with 0.5 mm inner diameter were used as a substrate for the antibody-immobilized column. Graft polymerization of acrylic acid onto the silicone tube surface was conducted as follows. The tube was treated with ozone gas (ON-3-2, Nippon Ozone Co., LTD., Tokyo, Japan) for 4 h, dipped in 10% acrylic acid/methanol solution, and incubated at 60 °C. After 4 h, the tube was washed with water [28,29]. Graft polymerization was confirmed by toluidine blue staining. To immobilize anti-CD34 antibody on the tube surface, the poly(-acrylic acid)-grafted tube was pre-activated with 1-ethyl-3-(3-dimethylaminopropyl) carbodiimide hydrochloride (WSC), filled with the anti-mouse CD34 rat IgG antibody (AbD Serotec) solution at concentration of 10 μg/ml, and incubated at 37 °C for 15 h. The tube was washed with PBS, treated with 1 mM 2-aminoethanol solution for 1 h, and preserved at 4 °C until experimental use. The column length was 10 cm, and the tilt angle was 20°.

2.4. Separation of crude MSCs on the antibody-immobilized column

A total of 2×10^4 cells of crude MSCs in 10 μL PBS were injected into the column. The column was flushed with PBS buffer at the flow rate of 50 μL/min until the flow

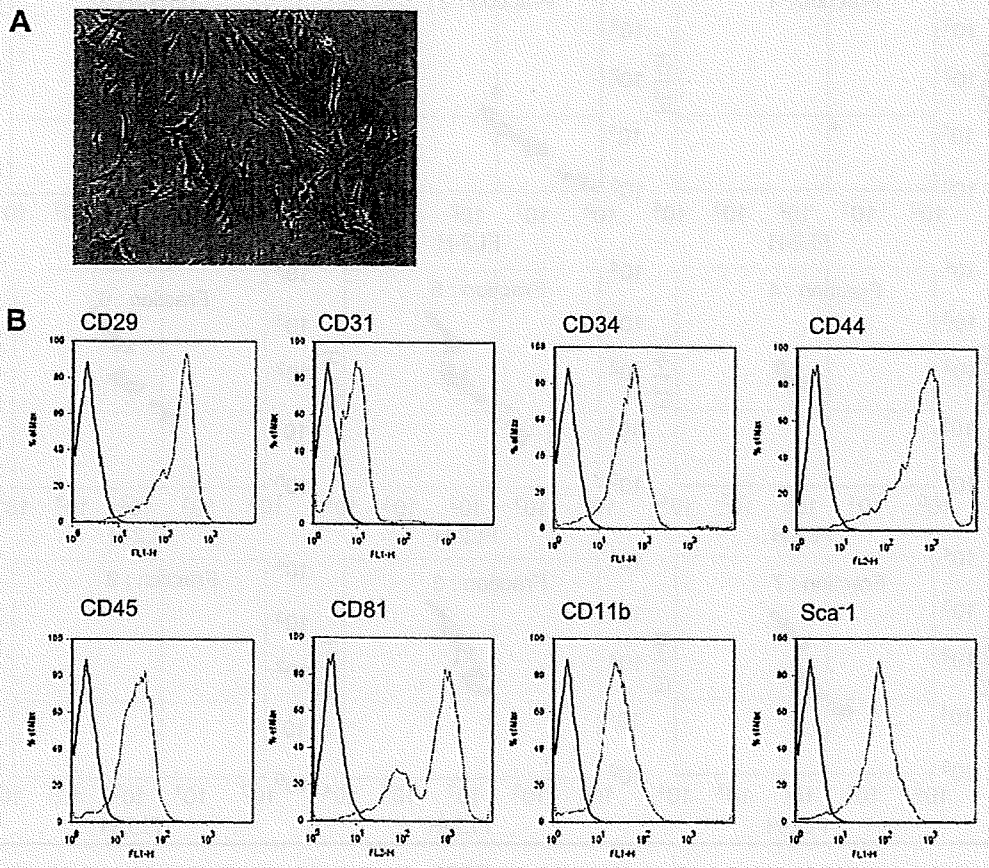

Fig. 1. (A) Morphology of murine MSCs culture. Cultured cells contained some type of cells like small round cells and fibroblast-like cells. (B) Surface marker expression of murine MSCs at passage 2. MSCs were stained with an FITC or PE-labeled antibody. Staining cells were shown in red histogram, and the black is unstained cells as control. These data were confirmed by 3 independent experiments.

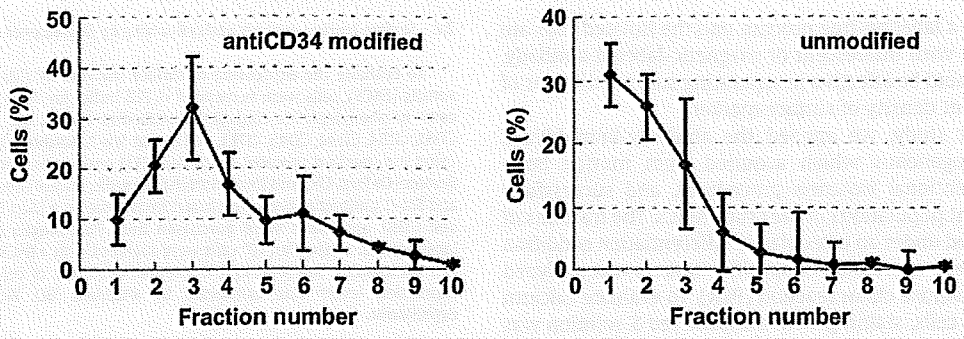

Fig. 2. Elution profiles of murine MSCs on the anti-CD34 antibody-immobilized column or unmodified column. Cell number ratio normalized by the total cell number was plotted against the fraction number. Each data point represents results from 3 independent experiment and the data are presented as mean ± standard error of the means.

volume of 250 μL, and at 600 μL/min thereafter. Eluted cell suspension was collected from top of the column, and cell suspensions were fractionated by elution volume (12.5 μL per fraction). Number and surface marker profile of cells in each fraction was analyzed by the FACS system.

2.5. Differentiation of isolated MSCs into osteoblasts

Purified MSC fractions were acquired from 2×10^4 crude MSCs. MSCs separated on the antibody-immobilized column were cultured on fibronectin-coated 24-well plates (FALCON, Oxnard, CA) with the osteoblastic differentiation medium containing 10^{-8} M dexamethasone, 10 mM β-glycerophosphate, and 0.3 mM ascorbic acid (all three reagents from Sigma–Aldrich, St. Louis, MO). The medium was changed 3 times per week. The cells were fixed with 10% formalin for 20 min at room temperature (RT) and stained with alizarin red S solution.

2.6. Gene expression analysis by real-time PCR

After culturing in differentiation medium for 1 week, total cellular RNA was isolated using Quickgene Mini80 with Quickgene RNA cultured cell kit S (FUJIFILM, Tokyo, Japan). Reverse transcription (ReverTra Ace, TOYOBO Co., LTD., Osaka, Japan) using oligo dT_{18} primer was performed on aliquots (200 ng) of total RNA as a template. The resultant cDNA was used for PCR amplification, and PCR analysis was

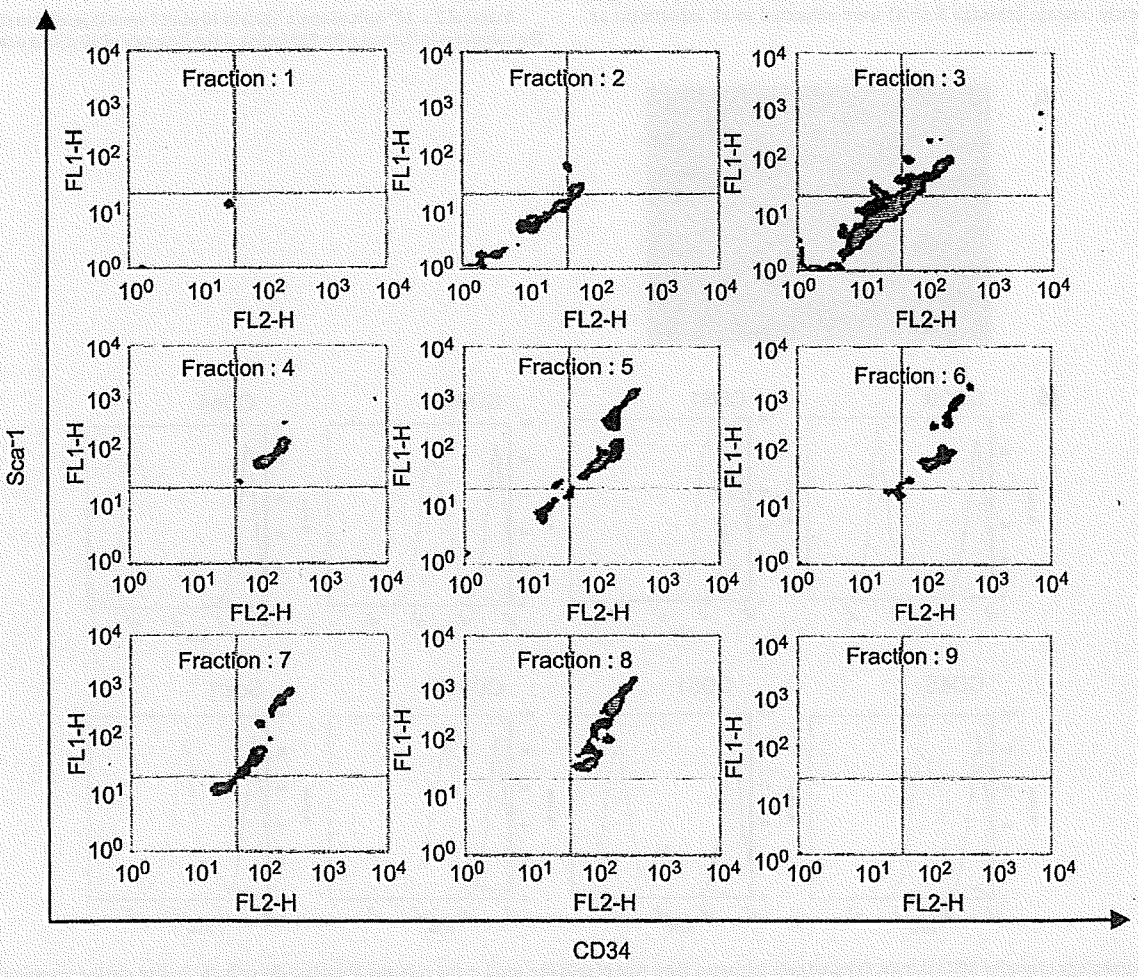

Fig. 3. Surface maker expression of isolated MSCs. Two-dimensional expression analysis of CD34 or Sca-1 was carried out in isolated cells fractions.

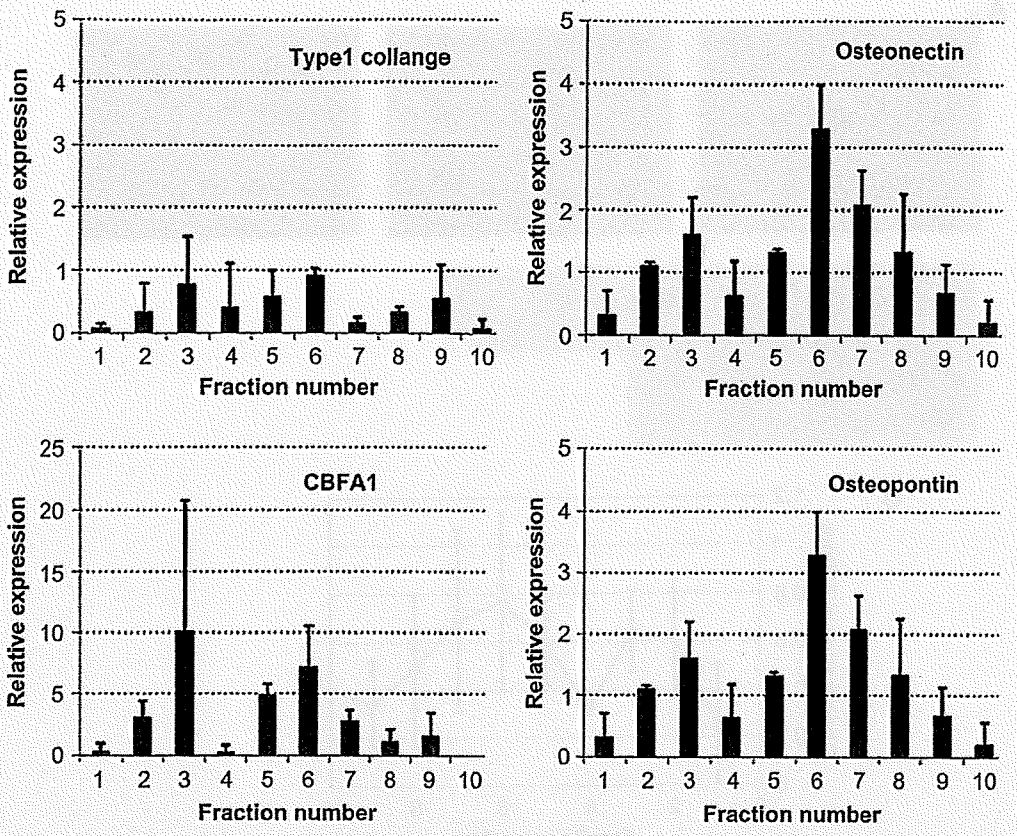

Fig. 4. Gene expression analyses of isolated MSCs on the anti-CD34 antibody-immobilized column for osteoblastic differentiation after 1 week. Relative expression is normalized by the expression of crude MSCs. GAPDH expression level was used as the internal standard control. Each data point represents results from 3 independent experiment and the data are presented as mean ± standard error of the means.

carried out by the GeneAmp 5700 Sequence Detection System (Applied Biosystems, Foster City, CA). PCR primers were designed by Primer Express software (Applied Biosystems). Type 1 collagen, CBFA1, osteopontin and osteonectin were selected as specific marker genes for differentiation. PCR reaction mixture contained 0.52 μL cDNA, 5 pmol of each primer, 25 μL SYBR Green Real-time PCR Master Mix (TOYOBO Co., LTD., Osaka, Japan). Amplification conditions were as follows: 40 cycles of 95 °C for 1 min; 60 °C for 15 s; 74 °C for 1 min. Primers used were (5′ to 3′) CBFA1: CCGCACGACAACCGCACCAT (forward), CGCTCCGGCCCACAAATCTC (reverse); Type 1 collagen: GAAGTCAGCTGCATACAC (forward), AGGAAGTCCAGGCTGTCC (reverse); Osteopontin: TCACCATTCGGATGAGTCTG (forward), ACTTGTGGCTCTGATGTTCC (reverse); Osteonectin: AGCGCCTGGAGGCTGGAGAC (forward), CTTGATGCCAAAG-CAGCCGG (reverse); GAPDH: CAAAATGGTGAAGGTCGGTGTG (forward), ATTT-GATGTTAGTGGGGTCTCG (reverse).

3. Results and discussion

3.1. Surface marker analysis of adherent cell population

MSCs are isolated by the bases of adherent property of bone marrow in some species, such as human [6] and rat [30]. However, it is difficult to isolate homogeneous MSCs by adhesion separation because of unwanted contamination. The crude MSCs displayed a fibroblast-like morphology shown in Fig. 1(A). To eliminate the monocytic cell fraction in adhesion cell population, magnetic beads conjugated with anti-CD11b or anti-CD45 antibodies were used for negative selection [14,16]. Although some surface markers for MSCs were reported in a recent study, homogeneous MSCs could not be identified by such kinds of markers [17,31]. Surface marker expression level of adherent population of murine MSCs are shown in Fig. 1(B). A strong expression of the surface markers CD29, CD44, CD81, and Sca-1, and a weak expression of the surface markers CD34, CD45, and CD11b were observed. No expression of CD31 was observed. Some studies have reported that murine MSCs were positive for the surface markers CD29, CD44 and Sca-1 [14,15,32], and this finding was confirmed in our experimental data. Sca-1 expression level changed with the culture period (data not shown). This phenomenon was already reported in other studies [32]. The MSCs showed a weak and broad expression of CD34, a hematopoietic lineage marker. Umezawa et al. reported that murine MSCs with a low expression of CD34 have a high potential for the regenerative effect in cardiopulmonary disease. CD34 is the progenitor or stem cell marker, and the expression continuously decreased with the culture period. That is, the CD34 expression would be closely related with the differentiation stage. Hence, we chose the anti-CD34 antibody as the immobilized ligand and evaluated the differentiation ability of MSCs isolated on the anti-CD34 antibody-immobilized column.

3.2. Separation profile of MSCs on the anti-CD34 antibody-immobilized column

We have developed a separation column in previous work [21]. Details about the separation column were shown in Materials and methods. The antibody-immobilized column was connected with an injection tube. The length of the column and injection tube was 100 mm. Medium flow into the column was accomplished with a syringe pump. Elution profile of crude MSCs on the anti-CD34 antibody-immobilized column was evaluated by counting the number of eluted cells in each fraction. When the crude MSCs were injected into an unmodified column, almost all the cells were eluted in early fractions. On the other hand, when the crude MSCs were injected into the anti-CD34 antibody-immobilized column,

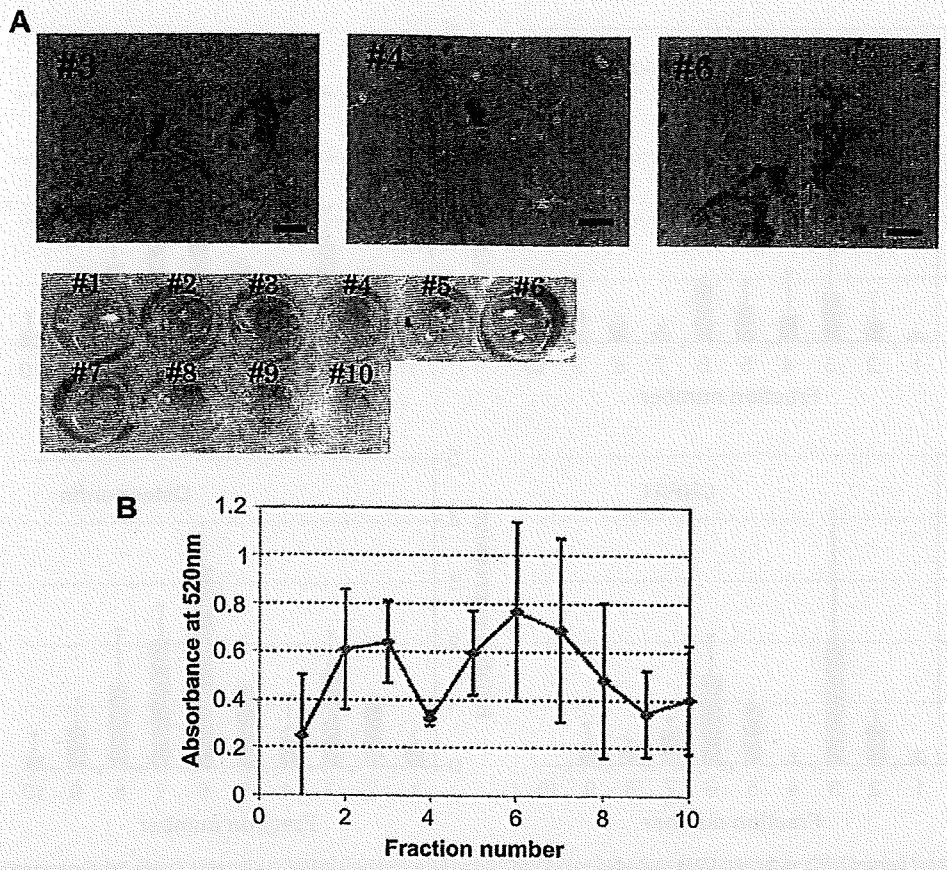

Fig. 5. (A) Photograph of alizarin red S staining MSCs after differentiation for 1 week. Cells were cultured on fibronectin-coated 24-well plate. (B) Quantification of alizarin red S staining in each fraction by absorbance spectrum. Absorption at 540 nm was plotted against the fraction number. Each data point represents results from 3 independent experiment and the data are presented as mean ± standard error of the means.

two peaks were observed (Fig. 2). That is, the delay of cell elution observed in the case of the anti-CD34 antibody-immobilized column probably resulted from the continuous interaction between the surface marker and the immobilized antibody. In our previous work, KG-1a (CD34+) and HL60 (CD34-) cells know as cell line were separated on antibody-immobilized column [21]. In the results, cells were separated by a marker specific manner, and the elution pattern was distinctly depended on the marker expression level. In the case of MSC separation, elution patterns were comparatively broad because of heterogeneity of crude MSCs. Then, surface marker expression of the isolated MSCs on the anti-CD34 antibody-immobilized column was evaluated by FACS. Two-dimensional FACS analysis of CD34 expression against Sca-1 expression is shown in Fig. 3. MSCs with a high expression of CD34 and Sca-1 were presented in later fractions, and a continuous change in the marker expression level was observed with increasing fraction number. These data indicated that the crude MSCs were separated on the column on the basis of the surface marker density. From the above results, we suggest that the antibody-immobilized column could be used to isolate murine MSCs on the basis of their surface marker density.

3.3. *Differentiation of isolated MSCs on the anti-CD34 antibody-immobilized column*

Osteoblastic differentiation was evaluated by gene expression analysis and alizarin red S staining. Type 1 collagen, osteonectin, CBFA1, and osteopontin were selected as specific markers for osteoblastic differentiation. The gene expression level was analyzed in separated MSCs obtained from the column. Type 1 collagen and osteonectin are constantly expressed during osteoblastic differentiation [33–35], while CBFA1 is expressed during the process of maturation. CBFA1 is a transcriptional factor, and the osteopontin expression was promoted by the CBFA1. Fig. 4 shows the expression levels of specific marker genes analyzed by real-time PCR. Type 1 collagen was expressed in almost all fractions, and the expression level was the same as that of crude MSCs. In the case of CBFA1, the expression level in fractions 3, 5, and 6 was higher than that in other fractions. This tendency was the same as that observed for the expression pattern of osteopontin.

CBFA1 is a key factor for mature osteoblastic differentiation. The suppression of CBFA1 expression by mutation of CBFA1 completely restricted bone formation of murine neonatal or newborn [33]. That is, the expression of CBFA1 is necessary for calcium deposition on the cells. The isolated MSCs after differentiation were stained with alizarin red S solution. Fig. 5 shows the picture of stained cells. Isolated MSCs in early fractions (fractions #2- and #3) or later fraction (fractions #5–7) were strongly positive. This staining pattern in terms of the fraction number was similar to that of CBFA1 expression pattern.

These results suggest that separated MSCs in early fraction or later fraction had a high potential for osteoblastic differentiation. It has been reported that osteoblastic progenitor cells were enriched in the CD34-positive population from bone marrow [36]. That is, the cells with high expression of CD34 in later fractions are mainly osteoblastic progenitor cells. It is difficult to determine the origin of these progenitor cells. However, there are two possibilities with

regard to their origin. First, the osteoblastic progenitor cells in bone marrow were contaminated in TCPS-adherent cells. Second, a fraction of MSCs differentiated into progenitor cells during cultivation. Stem cells are difficult to be cultured on a TCPS dish keeping with differentiation properties. Because the environment of MSCs on a culture dish is largely different from that *in vivo*, cultured MSCs have heterogeneous characteristics in terms of surface marker [17] and differentiation property. The purification process of stem cells is important for experimental or clinical use. From these results, we suggested that the ligand-immobilized column could be used to isolate MSCs from the heterogeneous cell populations consisting of progenitor or differentiated cells.

3.4. Differentiation of sorted MSCs by FACS

To verify the effect of surface marker density on the differentiation ability of MSCs, crude MSCs were sorted by FACS as a conventional method for cell separation. Four cell populations were sorted for the evaluation of osteoblastic differentiation (Fig. 6). The CD34 expression level in each population was different, and MSCs with a high density of CD34 were contained in $CD34^{High}FSC^{Low}$ population. In contrast, the low density of CD34 was collected in $CD34^{Low}FSC^{High}$ population. The surface marker density of the cells in $CD34^{High}FSC^{High}$ or $CD34^{Low}FSC^{Low}$ population was almost the same. Fig. 6(B) shows the relative expression of specific marker genes for osteoblastic differentiation. In case of MSCs sorted by FACS, cell population with high and low marker density of CD34 has shown high expression of differentiation markers. This tendency was the same as that observed for separated MSCs on the antibody-immobilized column. This result supported that the two cell populations with high ability for osteoblastic differentiation were present in crude MSCs, and the populations were separated using a CD34 antibody-immobilized column.

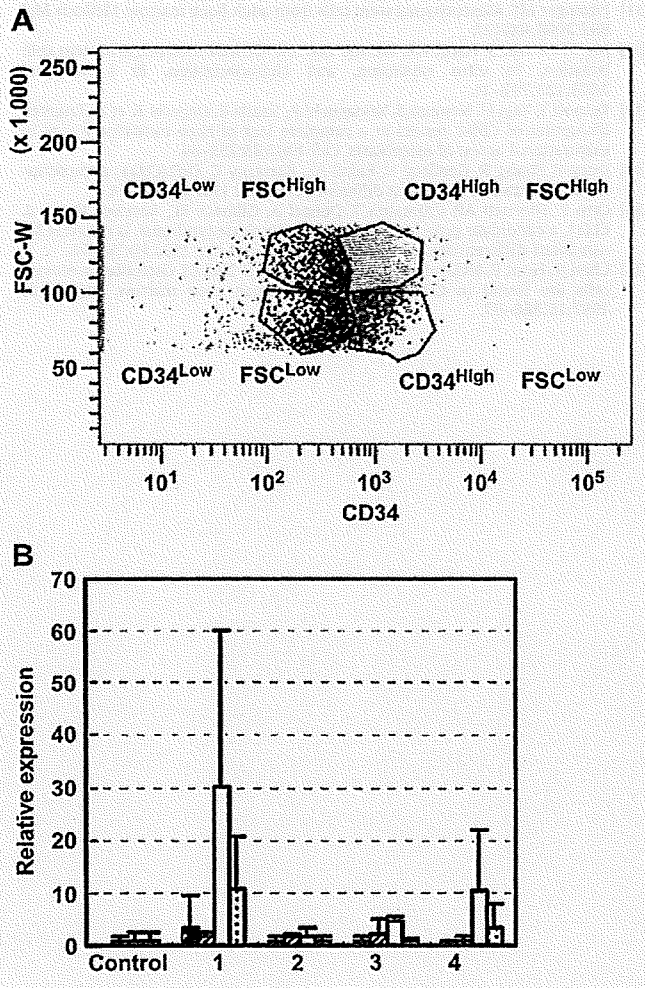

Fig. 6. (A) Sorting regions of isolated cell populations with distinct expression density. Crude MSC populations were divided into four cell populations. Cells with highest CD34 expression density were in the $CD34^{High}FSC^{Low}$ population. On the other hand, cells with lowest expression density were in the $CD34^{Low}FSC^{Hihg}$ population. (B) Gene expression analysis of sorted MSCs by FACS. Sorted MSCs were cultured in the osteoblastic differentiation medium for 8 days. Specific surface markers (bar with lines: type 1 collagen, bar with dots; osteonectin, closed bar; CBFA1, open bar; osteopontin) were analyzed by real-time PCR. Relative expression was normalized by GAPDH. Each data point represents results from 3 independent experiment and the data are presented as mean ± standard error of the means.

4. Conclusion

An anti-CD34 antibody-immobilized column was developed for separating MSCs based on their surface marker density. We selected the anti-CD34 antibody as the immobilized ligand, and crude MSCs were separated on this column. Two cell populations with a high ability for osteoblastic differentiation were purified on this column. MSCs express some surface markers, and their combinations have been explored in many groups in order to specify homogeneous MSCs population. In our approach, marker density is considered as the essential factor for the characterizing MSCs. Two different cell populations could be separated on this column based on their surface marker density. To characterize the cells with a high differentiation ability, it might be effective to use some kinds of ligand-immobilized columns. Further studies on the design of ligand-immobilized surface and construction of the column system are required for effective separation of MSCs.

Acknowledgment

This work was supported by the Research Grant for Cardiovascular Disease (18A-2) from the ministry of Health, Labour and Welfare & Grant-in-Aid for Scientific Research on Innovation Areas (20106014).

Appendix

Figures with essential colour discrimination. Most of the figures (Figs. 1, 3, 5 and 6) in this article have parts that may be difficult to interpret in black and white. The full colour images can be found in the on-line version, at doi:10.1016/j.biomaterials.2010.01.126.

References

[1] Langer R, Vacanti JP. Tissue engineering. Science 1993;260:920–6.
[2] Holden C, Vogel G. Plasticity: time for a reappraisal. Science 2002;296:2126–9.
[3] Kim SW, Han H, Chae GT, Lee SH, Bo S, Yoon JH, et al. Successful stem cell therapy using umbilical cord blood-derived multipotent stem cells for Buerger's disease and ischemic limb disease animal model. Stem Cells 2006;24:1620–6.
[4] Kim SS, Yoo SW, Park TS, Ahn SC, Jeong HS, Kim JW, et al. Neural induction with neurogenin1 increases the therapeutic effects of mesenchymal stem cells in the ischemic brain. Stem Cells 2008;26:2217–28.
[5] Fukuda K, Yuasa S. Stem cells as a source of regenerative cardiomyocytes. Circ Res 2006;98:1002–13.
[6] Pittenger MF, Mackay AM, Beck SC, Jaiswal RK, Douglas R, Mosca JD, et al. Multilineage potential of adult human mesenchymal stem cells. Science 1999;284:143–7.
[7] Yang IH, Kim SH, Kim YH, Sun HJ, Kim SJ, Lee JW. Comparison of phenotypic characterization between "alginate bead" and "pellet" culture systems as chondrogenic differentiation models for human mesenchymal stem cells. Yonsei Med J 2004;45:891–900.

[8] Lisignoli G, Cristino S, Piacentini A, Toneguzzi S, Grassi F, Cavallo C, et al. Cellular and molecular events during chondrogenesis of human mesenchymal stromal cells grown in a three-dimensional hyaluronan based scaffold. Biomaterials 2005;26:5677–86.
[9] Wan C, He Q, McCaigue M, Marsh D, Li G. Nonadherent cell population of human marrow culture is a complementary source of mesenchymal stem cells (MSCs). J Orthop Res 2006;24:21–8.
[10] Gronthos S, Zannettino AC, Hay SJ, Shi S, Graves SE, Kortesidis A, et al. Molecular and cellular characterisation of highly purified stromal stem cells derived from human bone marrow. J Cell Sci 2003;116:1827–35.
[11] Hung SC, Chen NJ, Hsieh SL, Li H, Ma HL, Lo WH. Isolation characterization of size-sieved stem cells from human bone marrow. Stem Cells 2002;20:249–58.
[12] Reyes M, Lund T, Lenvik T, Aguiar D, Koodie L, Verfaillie CM. Purification and ex vivo expansion of postnatal human marrow mesodermal progenitor cells. Blood 2001;98:2615–25.
[13] Jiang Y, Jahagirdar BN, Reinhardt RL, Schwartz RE, Keene CD, Ortiz-Gonzalez XR, et al. Pluripotency of mesenchymal stem cells derived from adult marrow. Nature 2002;418:41–9.
[14] Baddoo M, Hill K, Wilkinson R, Gaupp D, Hughes C, Kopen GC, et al. Characterization of mesenchymal stem cell isolated from murine bone marrow by negative selection. J Cell Biochem 2003;89:1235–49.
[15] Gojo S, Gojo N, Takeda Y, Mori T, Abe H, Kyo S, et al. In vivo cardiovasculogenesis by direct injection of isolated adult mesenchymal stem cells. Exp Cell Res 2003;288:51–9.
[16] Tropel P, Noël D, Platet N, Legrand P, Benabid AL, Berger F. Isolation and characterisation of mesenchymal stem cells from adult mouse bone marrow. Exp Cell Res 2004;295:395–406.
[17] Phinney DG, Hill K, Michelson C, DuTreil M, Hughes C, Humphries S, et al. Biological activities encoded by the murine mesenchymal stem cell transcriptome provide a basis for their developmental potential and broad therapeutic efficacy. Stem Cells 2006;24:186–98.
[18] Li Y, Zhang C, Xiong F, Yu MJ, Peng FL, Shang YC, et al. Comparative study of mesenchymal stem cells from C57BL/10 and mdx mice. BMC Cell Biol 2008;9:24.
[19] Wieczorek G, Steinhoff C, Schulz R, Scheller M, Vingron M, Ropers HH, et al. Gene expression profile of mouse bone marrow stromal cells determined by cDNA microarray analysis. Cell Tissue Res 2003;311:227–37.
[20] Matsuoka S, Ebihara Y, Xu M, Ishii T, Sugiyama D, Yoshino H, et al. CD34 expression on long-term repopulating hematopoietic stem cells changes during developmental stages. Blood 2001;97:419–25.
[21] Mahara A, Yamaoka T. Antibody-immobilized column for quick cell separation based on cell rolling. Biotechnol Prog, in press.
[22] von Andrian UH, Chambers JD, McEvoy LM, Bargatze RF, Arfors KE, Butcher EC. Two-step model of leukocyte-endothelial cell interaction in inflammation: distinct roles for LECAM-1 and the leukocyte beta 2 integrins in vivo. Proc Natl Acad Sci U S A 1991;88:7538–42.
[23] Eniola AO, Willcox PJ, Hammer DA. Interplay between rolling and firm adhesion elucidated with a cell-free system engineered with two distinct receptor-ligand pairs. Biophys J 2003;85:2720–31.
[24] Greenberg AW, Hammer DA. Cell separation mediated by differential rolling adhesion. Biotechnol Bioeng 2001;73:111–24.
[25] Greenberg AW, Brunk DK, Hammer DA. Cell-free rolling mediated by L-selectin and sialyl lewisx reveals the shear threshold effect. Biophys J 2000;79:2391–402.
[26] Hammer DA, Apte SM. Simulation of cell rolling and adhesion on surfaces in shear flow: general results and analysis of selectin-mediated neutrophil adhesion. Biophys J 1992;63:35–57.
[27] Hammer DA, Lauffenburger DA. A dynamical model for receptor-mediated cell adhesion of surfaces. Biophys J 1987;52:475–87.
[28] Fujimoto K, Takebayashi Y, Inoue H, Ikada Y. Ozone-induced graft polymerization onto polymer surface. J Polym Sci A Polym Chem 1993;31:1035–43.
[29] Yamauchi J, Yamaoka A, Ikemoto K, Matsui T. Graft copolymerization of methyl methacrylate onto polypropylene oxidized with ozone. J Polym Sci A Polym Chem 1991;43:1197–203.
[30] Wakitani S, Saito T, Caplan AI. Myogenic cells derived from rat bone marrow mesenchymal stem cells exposed to 5-azacytidine. Muscle Nerve 1995;18:1417–26.
[31] Pittenger MF. Mesenchymal stem cells from adult bone marrow. Methods Mol Biol 2008;449:27.
[32] Meirelles Lda S, Nardi NB. Murine marrow-derived mesenchymal stem cell: isolation, in vitro expansion, and characterization. Br J Haematol 2003;123:702–11.
[33] Komori T, Yagi H, Nomura S, Yamaguchi A, Sasaki K, Deguchi K, et al. Targeted disruption of Cbfa1 results in a complete lack of bone formation owing to maturational arrest of osteoblasts. Cell 1997;89:755–64.
[34] Ducy P, Zhang R, Geoffroy V, Ridall AL, Karsenty G. Osf2/Cbfa1: a transcriptional activator of osteoblast differentiation. Cell 1997;89:747–54.
[35] Otto F, Thornell AP, Crompton T, Denzel A, Gilmour KC, Rosewell IR, et al. Cbfa1, a candidate gene for Cleidocranial dysplasia syndrome, is essential for osteoblast differentiation and bone development. Cell 1987;89:765–71.
[36] Chen JL, Hunt P, McElvain M, Black T, Kaufman S, Choi ES. Osteoblast precursor cells are found in CD34+ cells from human bone marrow. Stem Cells 1987;15:368–77.

///VSP///

Journal of Biomaterials Science 0 (2010) 1–14

Journal of BIOMATERIALS SCIENCE
brill.nl/jbs

Peripheral Nerve Regeneration and Electrophysiological Recovery with CIP-Treated Allogeneic Acellular Nerves

T. Ehashi [a], A. Nishigaito [a,b], T. Fujisato [a,c], Y. Moritan [b] and T. Yamaoka [a,*]

[a] Department of Biomedical Engineering, National Cardiovascular Center Research Institute, 5-7-1 Fujishiro-dai, Suita, Osaka 565-8565, Japan

[b] Department of Medical Engineering, Suzuka University of Medical Science, Suzuka, Japan

[c] Department of Biomedical Engineering, Osaka Institute of Technology, Osaka, Japan

Received 30 October 2009; accepted 19 January 2010

Abstract

Acellular nerve grafts are a desirable alternative to autografts, both because the source of acellular nerves is potentially unlimited and because they have the same matrix structure as natural nerves, which would facilitate axon growth from the defective nerve stump. Although some acellular nerves have been developed, most of them were studied in isogenic transplantation models and evaluated only by histological observation. In the present study, novel allogeneic acellular nerves prepared using the cold isostatic pressing (CIP) method were developed and assessed as a potential substitute for autografts. The host immune response to acellular nerves and fresh nerves was analyzed using Lewis rats as donors and SD rats as recipients, which is the allogeneic transplantation model, by subcutaneous implantation for one month. In addition, sciatic nerve transplantation into a 10-mm nerve gap was carried out using the same model, and the axonal growth in acellular nerve transplantation was evaluated histologically and electrophysiologically, and compared with that of axons in the autograft transplant area. The subcutaneously implanted acellular nerves contained more macrophages and less vasculature than the allogeneic fresh nerves. In spite of these results of the subcutaneous implantation, Schwann cell infiltration in the graft transplanted into the sciatic nerve gap was observed after the short-term transplantation. The myogenic potential, which was measured as an index of electrophysiological function in acellular nerve transplantation, was also recovered in the long-term transplantation. Our results indicate that the acellular nerves developed herein have the potential to support nerve regeneration and might be useful as an alternative to autografts.

Keywords

Acellular nerve, allogeneic, electrophysiological study, cold isostatic pressing treatment

* To whom correspondence should be addressed. Tel.: (81-6) 6833-5012; Fax: (81-6) 6835-5476; e-mail: yamtet@ri.ncvc.go.jp

DOI:10.1163/092050610X488250

1. Introduction

Autologous fresh nerves are commonly used in clinical applications for treating peripheral nerve defects. However, an alternative to the autologous nerves is needed because these nerves are available only in limited quantities, and also because their use causes concurrent healthy nerve dysfunction [1, 2]. In general, tissue-derived nerves are always preferable, since they possess a natural internal structure of extracellular matrix components, which can lead to cellular migration and nerve fiber elongation [3–7].

Cadaveric donor grafts are an attractive alternative to autologous nerves, and their supply is potentially unlimited. In 2001, clinical trials for cold-preserved nerve allografts were reported to cause severe peripheral nerve defects [8]. In that report, 6 patients exhibited successful nerve reconstruction by cadaveric nerve allograft transplantation. However, long-term systematic administration of immunosuppressant was required, and even with that degree of treatment, one of the patients still experienced immune rejection. Moreover, it has been reported that the rate of nerve regeneration using cold preserved allogeneic nerves is lower than that using autologous fresh nerves with immunosuppressant treatment [9].

For treatment without an immunosuppressant, various strategies to eliminate the immunogenicity of allogeneic nerves have been explored in different animal models, but the grafts revealed very poor completeness in comparison to that of the autografts [10–12]. The main strategies for reducing the immunogenecity of allografts or xenografts are thermal and chemical pretreatments of nerves [8, 13, 14]. These pretreatments can destroy or remove the donor cells, but the natural internal structure of the nerve tissue remains unchanged.

The thermal process involves repeated cycles of freezing and thawing of donor nerves. This process destroys the allogeneic antigen and eliminates allogeneic cells, and has been reported to decrease the host antigeneic response in some studies [8, 15]. However, the axonal growth in these grafts is slower than it is in fresh autografts or isogeneic grafts, because of the residual allogeneic cells in the graft [13]. The cellular debris in the graft leads to macrophage invasion and basal laminae damage, which delay the nerve regeneration [16–19].

Chemical processes to remove the donor cells with detergents have been studied not only for peripheral nerve tissue [14, 20, 21] but also for cardiac muscle [22], heart valves [23] and pericardium [24]. This process is more effective in removing the donor cells. However, it also causes more damage to the extracellular matrices than thermal pretreatment does [7, 25, 26]. In addition, it is difficult to completely remove the detergent from the graft, and the residual chemicals suppress tissue regeneration. Starting in 2002, decellularized human nerves which are processed with a combination of detergent decellularization, chondroitinase degradation and gamma-irradiation sterilization have been marketed by AxoGen in the US. The decellularized nerve grafts are superior to the commercially available conduits but not as effective as isografts [27].

We have established a novel decellularization method using a cold isostatic pressing (CIP) treatment [28]. This method has succeeded in removing the cellular components from pig blood vessels, heart valves and trachea. We have also reported on the excellent reconstruction of endothelial cells, fibroblasts and smooth muscle cells in acellular vessels 12 weeks after the transplantation [28]. Thus, novel allogeneic acellular nerve grafts that possess natural extracellular matrices were prepared by the CIP method and examined in this study. In fact, many studies have been performed to develop novel treatments as an alternative to autografts, and most of the acellular tissue transplantations have been studied using isogeneic transplantation models [2, 20, 29, 30]. However, only a few studies have focused on allogeneic transplantation [8, 21, 26, 31]. Moreover, the regeneration of nerves by pretreated nerve transplantation should be assessed functionally in addition to histologically. For example, there have been only a few studies focused on the conduction velocity [20, 32] or myogenic potential [20, 31] of the acellular nerve transplantation. Therefore, for this study, allogeneic acellular nerves were prepared from Lewis rat sciatic nerves, and transplanted into a sciatic nerve gap in SD rats. As a preliminary study, a 10-mm gap of sciatic nerve which is repaired by any other nerve graft substitute, was bridged with our acellular nerve grafts to evaluate their potential in nerve regeneration, and the axonal growth in the allogeneic acellular nerves was evaluated histologically and electrophysiologically.

2. Materials and Methods

2.1. Preparation of Acellular Nerves

All animal studies were performed in accordance with the guidelines of the Ministry of Health, Labour and Welfare of Japan, as well as the guidelines of our institution, and approved by the Institutional Animal Care and Use Committee at the National Cardiovascular Center Research Institute.

Approximately 30-mm lengths of the sciatic nerves were harvested from a male Lewis rat weighing 300–350 g (Japan SLC) and, after trimming their peripheral fat and connective tissues, the nerves were packed in a polyethylene pouch with Ca^{2+}-, Mg^{2+}-free phosphate-buffered saline (PBS; Invitrogen) and the air was expelled. The nerves were then treated with ultra high pressure of 980 MPa at 30°C for 10 min using a Dr. Chef high pressure food processor (Kobe Steel) to disrupt all cells, microorganisms, and viruses inside the tissues. The cell debris was washed away by immersing the cells in endothelial cell growth medium (EGM-2 Bulletkit; Lonza) for 2 weeks at 37°C. Then, ethanol/PBS (80:20, v/v) was used to remove phospholipids, which lead to calcification of implants, and was removed by rinsing with PBS for 3 days.

The acellular nerves were morphologically and histologically compared with the untreated nerves. The decellularization efficiency and extra-cellular component morphology were evaluated by hematoxylin and eosin staining (HE staining). Briefly, the samples were fixed with 10% neutralized formalin, then dehydrated and

embedded in paraffin, sectioned at 8–10 μm, and captured on slide glasses. The slide glasses were immersed into Mayer's hematoxylin solution (Wako), rinsed with tap water, and counterstained with eosin solution (Wako).

2.2. *Subcutaneous Implantation*

The host body reaction to the allogeneic fresh nerves and allogeneic acellular nerves was investigated by subcutaneous implantation into rats. As the allogeneic transplantation model, we used Lewis rats and SD rats as donor and recipient animals, as described by Hudson *et al.* [17]. Three 13-week-old male SD rats (Japan SLC) were anesthetized with isoflurane inhalation. Two incisions were made in the dorsal skin on the back of each of three SD rats, and fresh or acellular nerves of a Lewis rat (10 mm long) were inserted into both subcutaneous spaces. Thus, one fresh nerve sample and one acellular nerve sample was implanted into the back of each of the three rats. After 4 weeks of implantation, all rats were killed humanely and the grafts were resected with the surrounding skin.

Angiogenesis and macrophage infiltration against the grafts was evaluated by HE staining ($n = 3$) and immunostaining for von Willebrand Factor (vWF) ($n = 1$) and CD68 ($n = 3$). All resected tissues with graft were fixed with 10% formalin, dehydrated with gradient alcohol and embedded in paraffin. All nerves were sectioned at 4 μm thickness and the middle parts of the grafts were used for staining. For the primary antibody, anti-vWF antibody (Dako) and anti-CD68 antibody (AbD Serotec) were used, and horseradish peroxidase-conjugated secondary antibody (Dako), 3,3-diaminobenzidine substrate (Dako) and eosin solution (Wako) were used to visualize the cells.

The total numbers of infiltrated cells and macrophages in implants and the number of blood vessels with a luminal structure were calculated. The total numbers of cells and macrophages were analyzed using free imaging soft, ImageJ (NIH). Pictures were taken at 40× magnification, and the numbers of nuclei and stained cells were counted using particle analysis tools included in the software package. In HE staining and immunostaining for CD68, three areas were randomly selected within implanted nerves. Blood vessels with a circular form with vWF positive cells inside the grafts were counted visually.

2.3. *Implantation of Graft in the Sciatic Nerve Defect*

The allogeneic acellular nerves prepared by CIP treatment were transplanted to rat sciatic nerve defect models. The recipient animals, 6 SD rats, were anesthetized by isoflurane, and both sides of the sciatic nerves were exposed. A 10-mm length of the right-side sciatic nerve was excised, and an acellular nerve graft of the same length was sutured at both stumps of the recipient nerve using 10-0 vicryl (Ethicon) under a microscope. Another side sciatic nerve was excised, and the excised nerve was reversed and sutured in the same way as the autograft control. Four of the transplanted animals underwent electrophysiological and histological study, and the others were only used for histological evaluation.

2.4. Assessment of the Transplanted Nerves

The transplanted grafts were electrophysiologically evaluated by electromyogram in short-term (158 days; $n = 1$) and long-term (247, 248 and 258 days; $n = 1$ each) experiments. Under anesthesia, both sides of the sciatic nerves were exposed from the proximal to the distal parts of the graft positions. The proximal part of the nerve was hooked with two platinum wire electrodes and stimulated with 1 V monophagic rectangular voltage with 10 μs duration at a frequency of 1 Hz (Nihon Koden). The myogenic potential of the tibial muscle group was recorded by inserting two needle-type electrodes, amplified (Nihon Koden), and acquired by a PowerLab system (AD Instruments). In all cases, 50 traces were recorded and averaged.

In the histological evaluation, sciatic nerves including the graft were resected at 110 days ($n = 1$) and 158 days ($n = 1$) post-operation. The nerves were fixed with 10% neutralized formalin, dehydrated, and embedded in paraffin. Then, the tissues were sliced longitudinally in sections of 4 μm thickness each, and the middle parts of the grafts were stained using HE or anti-glial fibrillary acidic protein (GFAP) antibody (Dako), which stains Schwann cells in peripheral nerves. The anti-GFAP was visualized with labeled polymer (Dako) according to the manufacturer's specifications. Hematoxylin staining (Wako) was carried out as a counterstaining measure to visualize the nuclei.

2.5. Statistical Analysis

The total number of cells and macrophages in the subcutaneous implantation experiments was counted. The mean values of all parameters were determined along with their standard deviations. Student's t-tests were applied to determine the statistical significance of differences between numbers of total cells and macrophages in allogeneic fresh or allogeneic acellular grafts. Values of $P < 0.05$ were considered to indicate statistical significance.

3. Results

3.1. Decellularization of Rat Sciatic Nerves

Acellular rat sciatic nerves were prepared by destroying cells using CIP treatment and a washing process. At two time points, i.e., immediately after CIP treatment or after CIP treatment plus 3 weeks of washing, nerves were histologically compared with untreated fresh nerves by hematoxylin and eosin (HE) staining and immunostaining for GFAP (Figs 1 and 2). The results showed that CIP treatment alone could not remove the cells (Fig. 1B). After the washing process, all cells were removed from the tissue, and fiber-like extracellular matrices (ECM) were left behind (Fig. 1C). On the other hand, there were many nuclei present among the dense matrices in the untreated fresh nerves (Fig. 1A). Immunostaining showed that the Schwann cells in the nerves completely disappeared after decellularization (Fig. 2B). These histological observations showed that the decellularization process

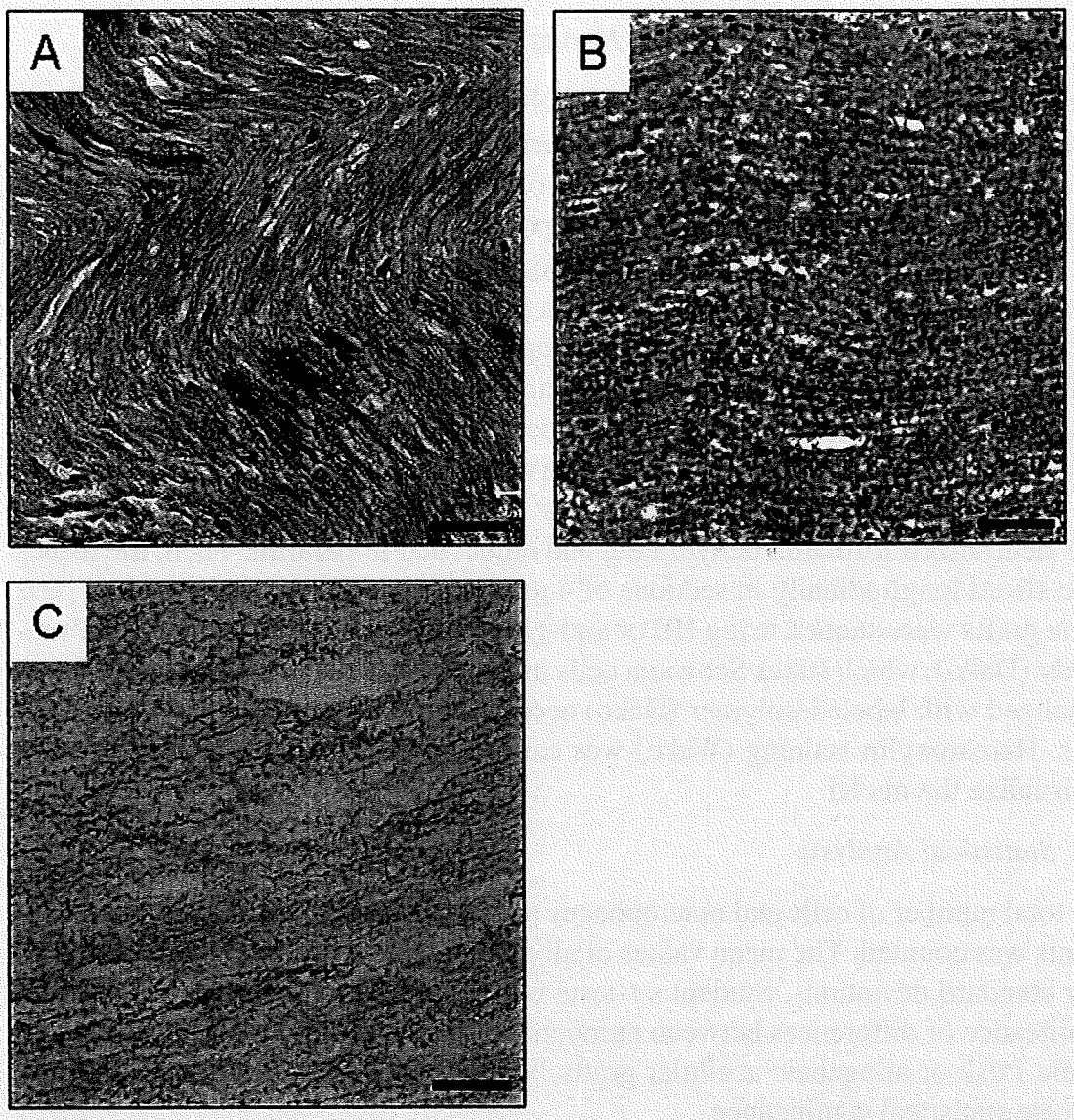

Figure 1. HE staining of a fresh nerve (A), a nerve just after CIP treatment (B) and a nerve after the complete washing process (C). Scale bars = 50 μm.

succeeded in the removal of cellular components while retaining the nerve ECM. The remaining ECM maintained an intrinsic orientation that is expected to be effective for axonal growth.

3.2. Host Body Reactions Against Allogeneic Fresh and Acellular Nerves

To investigate how the decellularization process affects the host body reaction, fresh and acellular nerves of Lewis rats were implanted subcutaneously into the SD rats and assessed histologically. At 1 month post-operation, many cells had infiltrated in both grafts (Fig. 3). However, the cell shapes were quite different between the fresh nerve and the acellular nerve. Many cells in the fresh nerve showed spindle-shaped nuclei and cytoplasms, whereas round shapes were seen in the acellular nerve (Fig. 3A and 3B). Immunostaining for CD68 showed that most cells in the

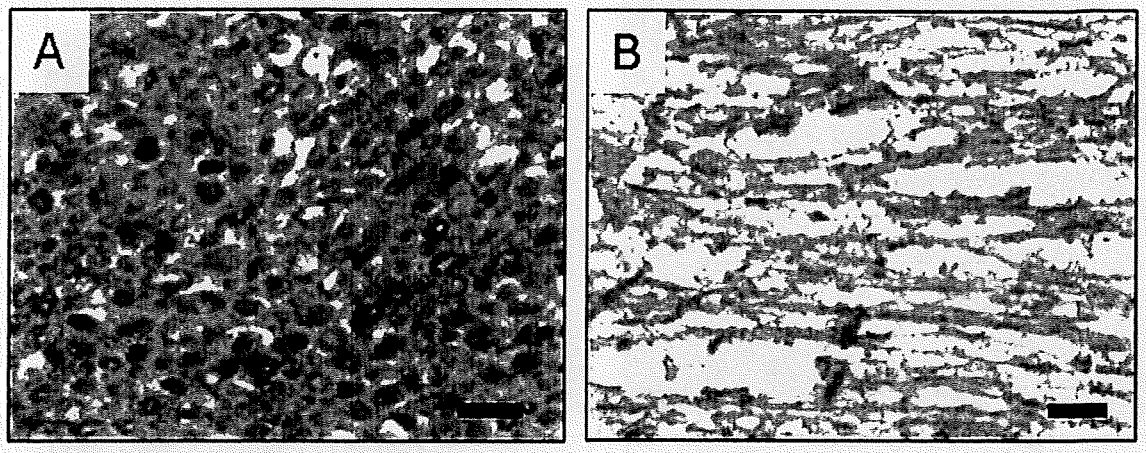

Figure 2. Immunostaining for GFAP of fresh (A) and acellular (B) nerves before implantation. Scale bars = 50 μm.

acellular nerves were macrophages while there were very few CD68-positive cells in the fresh nerves (Fig. 3C and 3D). The total numbers of cells and CD68-positive cells are summarized in Fig. 4. The total cell densities in the fresh and acellular nerves were the same. However, most cells in the acellular nerves were CD68-positive cells, whereas there were almost no CD68-positive cells in the fresh nerves. The major cell population in the fresh nerves could not be identified from immunostaining.

Angiogenesis in the graft was visualized by vWF immunostaining (Fig. 3E and 3F). When the fresh nerve was implanted, many small capillaries were present inside the graft (495 capillaries), and the surrounding subcutaneous tissue had normal vessels. On the other hand, when the acellular nerve was implanted, angiogenesis did not occur in the graft (19 capillaries), but blood vessels with a larger diameter did appear in the surrounding tissues. These observations suggest that the decellularization process might have changed the characteristics of the nerves and caused a different host body reaction in comparison to that elicited by the fresh nerves.

3.3. Histological Evaluation of the Acellular Nerve Grafts

Histological evaluation of the transplanted grafts was carried out by HE staining and immunostaining for GFAP on 110 days and 158 days after the operation (Fig. 5). Both in the fresh autograft and in the acellular allogeneic graft, remarkable cellular infiltration was observed by HE staining, even at 110 days after transplantation. Most of these cells were aligned in the longitudinal direction of the nerves, but rarely formed a fiber-like morphology at that point on time. On the other hand, 158 days after transplantation, many fibrous structures in the long-term transplantation were observed, especially in the autologous fresh nerve.

Immunostaining for GFAP in the Schwann cells in the peripheral nerves showed that the Schwann cells had infiltrated the host nerves. At 110 days post-operation,